

Calculation of ^{125}Te Chemical Shifts Using Gauge-Including Atomic Orbitals and Density Functional Theory

Yosadara Ruiz-Morales, Georg Schreckenbach, and Tom Ziegler*

Department of Chemistry, The University of Calgary, Calgary, Alberta, Canada T2N 1N4

Received: January 6, 1997; In Final Form: March 12, 1997[⊗]

Calculations of ^{125}Te nuclear magnetic resonance chemical shifts are reported for a number of organic, inorganic, and organometallic tellurium-containing complexes. The selected systems cover almost the complete spectrum of known ^{125}Te chemical shifts with a range of about 3000 ppm. The calculations are based on density functional theory (DFT) and gauge-including atomic orbitals (GIAO's). It is concluded that the DFT-GIAO method is able to reproduce the observed trends in ^{125}Te chemical shifts for organic, inorganic, and organometallic compounds.

1. Introduction

The shielding tensor of nuclear magnetic resonance (NMR) spectroscopy is probably one of the most important second-order response properties^{1–5} of molecular spectroscopy. Much progress has been achieved in the last decade toward a correct description of the shielding by first-principles electronic structure theory. Calculations of the shielding have been carefully reviewed in an annual series.⁶ A good survey of the state of the art can be found in a recent volume of conference proceedings.⁴ Some of the most important developments of the last few years comprise the inclusion of electron correlation into shielding calculations.^{3,4,6–8}

Much of the theoretical work so far has focused on compounds of “light” elements such as hydrocarbons, despite the rapidly growing experimental significance of multinuclear NMR.⁹ It is only recently that the range of theoretically accessible nuclei has been extended to gradually include the compounds of heavier elements as well. Such calculations, on various levels of theory, are still comparatively rare.^{10–15} This is not too surprising since such heavy element compounds pose additional difficulties on top of the—already challenging—task of computing the shielding. First, there is the large number of electrons that have to be taken into account. However, more important is the influence of special relativity.^{16,17}

We have recently presented a method in which the NMR shielding tensor is calculated by combining the “gauge-including atomic orbitals” (GIAO) approach with density functional theory (DFT).^{18,19a} An investigation²⁰ on a number of selenium-containing compounds has shown that our scheme is able to predict ^{77}Se chemical shift as well as individual tensor components of the ^{77}Se shielding tensor with about the same accuracy as sophisticated *ab initio* methods. In this investigation use was made of a newly developed scheme in which the GIAO-DFT method was extended to include the frozen core approximation.²¹

The purpose of the present study is to test the performance of the DFT-GIAO method for the even heavier fourth-row main group compounds. In the present paper, we apply our method to the calculation of the ^{125}Te chemical shifts of various organic, inorganic, and organometallic tellurium-containing complexes. Since relativity might be of importance, use will be made of a recently implemented scheme in which the frozen core DFT-GIAO method has been extended to include the scalar relativistic

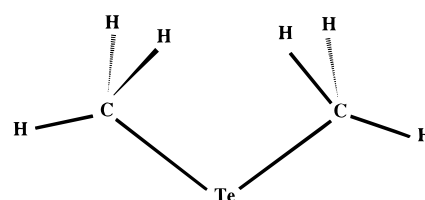


Figure 1. Staggered–staggered conformation of $\text{Te}(\text{CH}_3)_2$.

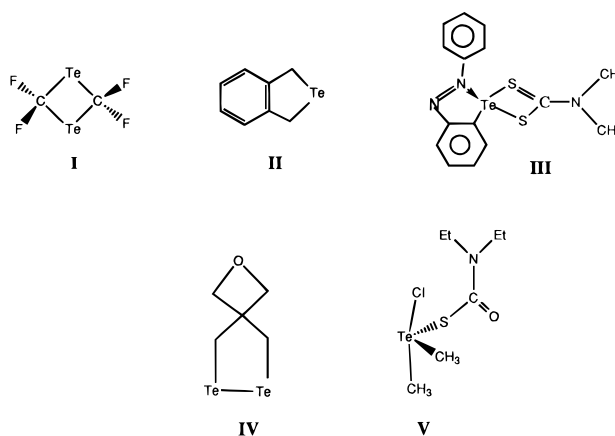


Figure 2. Structures for some of the organotellurium compounds.

two-component Pauli type Hamiltonian.²² Our calculations do not consider spin–orbit effects. We are presently carrying out the implementation of spin–orbit coupling into our DFT-GIAO method. There are no other calculations of ^{125}Te chemical shifts reported in the literature, so the DFT-GIAO method cannot be tested against other theoretical approaches as it is the case for ^{77}Se calculations.

2. Computational Details and the GIAO-DFT Method

Our implementation of the DFT-GIAO method has been described in detail elsewhere.^{18,20–22} All the calculations were carried out with inclusion of relativity. They are based on the Amsterdam density functional package ADF.^{23–28} We use experimental geometries, unless otherwise stated. More complex structures are shown schematically in Figures 1–3. The exchange–correlation (XC) energy functional according to Becke²⁹ and Perdew³⁰ is employed on top of the local density approximation, LDA.

The 1s shells of carbon, nitrogen, oxygen, and fluorine are considered as core and are kept frozen. A total of seven valence

[⊗] Abstract published in *Advance ACS Abstracts*, May 1, 1997.

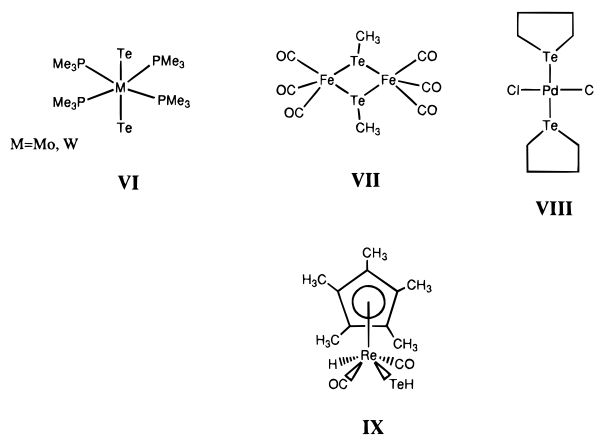


Figure 3. Structures for some of the organometallic tellurium compounds.

electrons were considered for chlorine and bromine, while the core of tellurium contains the 1s, 2s, 2p, 3s, 3p, 3d, 4s, and 4p shells.

We employ an uncontracted triple- ζ -quality valence basis of Slater type atomic orbitals (STOs).³⁴ The valence region of the basis is extended by two sets of d (p for hydrogen) polarization functions per atomic center. This type of basis set used here is of the same quality as the basis used in our previous study of ⁷⁷Se shielding constants.²⁰

The NMR shielding tensor for nucleus N can be written as¹⁸

$$\sigma_{\lambda\nu} = \sigma_{\lambda\nu}^d + \sigma_{\lambda\nu}^p = \int \frac{\vec{r}_N \times [\vec{J}_\nu^d(\vec{r}_N) + \vec{J}_\nu^p(\vec{r}_N)]_d}{r_N^3} d\vec{r}_N \quad (1)$$

Here \vec{J}^d and \vec{J}^p are respectively the diamagnetic and paramagnetic current densities¹⁸ induced by an external magnetic field \vec{B}_0 . The paramagnetic current density originates primarily from a coupling between occupied, Ψ_i , and virtual orbitals, Ψ_a , induced by the external magnetic field \vec{B}_0 :

$$\vec{J}^p = \sum_{s=1}^3 \sum_i^{\text{occu}} \sum_a^{\text{occ}} u_{ai}^{(1,s)} [\Psi_i \nabla \vec{\Psi}_a - \Psi_a \nabla \vec{\Psi}_i] B_{0,s} \quad (2)$$

The principle contribution to the coupling $u_{ai}^{(1)}$ is given by

$$u_{ai}^{(1)} \propto - \frac{1}{2(\epsilon_i^{(0)} - \epsilon_a^{(0)})} \sum_{\lambda,\nu} c_{\lambda a}^{(0)} c_{\nu i}^{(0)} \{ \langle \chi_\lambda | [\vec{r}_\nu \times \vec{\nabla}]_u | \chi_\nu \rangle \} \\ \propto - \frac{1}{2(\epsilon_i^{(0)} - \epsilon_a^{(0)})} \langle \Psi_a | \hat{M}_u | \Psi_i \rangle \quad (3)$$

Here $\epsilon^{(0)}$ refers to orbital energies of the unperturbed molecules without the external field.

Within the GIAO formalism,¹⁸ the action of the magnetic operator \hat{M}_u on Ψ_q is simply to work with $i\hat{L}_u^\nu$ on each atomic orbital x_ν . Here \hat{L}_u^ν is the u -component of the angular momentum operator with its origin at the center \vec{R}_ν on which x_ν is situated. Tabulations for $\hat{L}_u^\nu x_\nu$ are available in the literature.^{19b,c}

3. Results and Discussions

A. Absolute Shieldings and Relative Shifts. A direct comparison between calculated and observed shieldings would constitute the most straightforward and thorough validation of the DFT-GIAO scheme. Such a comparison is only possible

for elements where an experimental absolute shielding scale exists. This is the case for the ¹²⁵Te probe. Thus, Jameson and Jameson³¹ determined the tellurium shielding in TeF₆ to be 3790 ± 130 ppm. This result made it possible to estimate the absolute isotropic shielding constant for the ¹²⁵Te reference molecule Me₂Te as 4333 ppm³¹ and thus establish an absolute scale for ¹²⁵Te.

However, the experimental value by Jameson and Jameson³¹ relies by necessity on a theoretical determination of the diamagnetic shielding for the free tellurium atom. To this end, Jameson and Jameson carried out a nonrelativistic calculation on the diamagnetic shielding for the free tellurium atom and added an estimated relativistic correction. Their nonrelativistic value of 5362 ppm is in excellent agreement with our nonrelativistic shielding constant calculated as 5365 ppm. On the other hand, their estimated relativistic correction, due to the contraction of the core density,¹⁶ of 1220 ppm, is far larger than the relativistic correction of 275 ppm obtained by us from an actual calculation using a fully relativistic Dirac-DFT program for the atomic calculations, Table 1. Our calculations would indicate that the absolute scale due to Jameson and Jameson should be reduced by 945 ppm.

The experimentally accepted standard for ¹²⁵Te chemical shifts is dimethyl telluride, (CH₃)₂Te. We have therefore included it in our investigations. The experimental structure of this compound has been determined in the gas phase, on the basis of electron diffraction.³² The conformation around the C–Te bonds is found to be staggered–staggered, which is pseudo-cis with respect to the two methyl groups, Figure 1. Thus, the C_{2v} conformation was used for the calculation of the theoretical reference for relative shifts.

Calculated absolute shielding constants for a number of molecules are presented in Table 1. Here we investigated the influence of the inclusion of relativity as compared with nonrelativistic calculations. There are a few points to note about the results in Table 1. First, the maximal changes due to the inclusion of relativity are 182.1 and 188.1 ppm for (CH₃)₂Te and TeF₆, respectively. This means that relativity has a notable effect on the calculated absolute shielding, whereas part of the relativistic effects cancel in (relative) chemical shifts.

Furthermore, we note from Table 1 that relativity increases the calculated absolute chemical shieldings. This is a direct result of the relativistic contraction of the core density, which in turn produces a higher diamagnetic contribution to the shielding. For example, in the case of the tellurium atom only the diamagnetic shielding is important, and we calculate a change of 275 ppm in the absolute shielding between the nonrelativistic and the relativistic calculations, Table 1. The effects of the inclusion of relativity can be observed only in the absolute chemical shielding because these effects cancel in (relative) chemical shifts. For example a change of only 6.2 ppm between the nonrelativistic and the relativistic calculations is observed for TeF₆ if the relative chemical shift is considered instead of a change of 188 ppm when the absolute chemical shielding is analyzed. In terms of the relative chemical shifts the diamagnetic chemical shift has a small contribution to the total chemical shift.

Finally, after a reduction of the absolute scale for ¹²⁵Te of 945 ppm, the calculated relativistic shielding constants are within 300 ppm of the experimental estimates, Table 1. We decided to include relativity in all our calculations due to the facts presented and discussed in Table 1.

B. ¹²⁵Te Chemical Shifts. Calculated ¹²⁵Te chemical shifts for our DFT-GIAO method are included in Tables 2, 4, and 6

TABLE 1: Calculated and Experimental Absolute Shielding Constants and Chemical Shifts for Selected Tellurium-Containing Molecules, Including the Reference $(\text{CH}_3)_2\text{Te}$

| system | ^{125}Te absolute shielding (ppm) | | | ^{125}Te (relative) chemical shift (ppm) | | |
|---------------------------------------------------------------|--------------------------------------------------------------|-----------------|--------------|---------------------------------------------------|-----------------|--------------|
| | experimental | calculated | | experimental | calculated | |
| | | nonrelativistic | relativistic | | nonrelativistic | relativistic |
| Te atom | 6582 ^s , (5362) ^f 5637 ^j | 5365 | 5640 | | -2496.8 | -2589.7 |
| $(\text{CH}_3)_2\text{Te}$, staggered-staggered ^b | 4333 ^a , 3388 ^j | 2868.2 | 3050.3 | 0.0 | 0.0 | 0.0 |
| TeF_6 ^c | 3790 ± 130 ^a 2845 ± 130 ^j | 2260.0 | 2448.1 | 545.0 ^h | 608.2 | 602.0 |
| $[\text{TeCl}_6]^{2-}$ ^c | | 1680.1 | 1737.2 | 1531.0 ^h | 1188.1 | 1313.0 |
| $\text{Te}(\text{CH}_3)_4$ ^d | | 3018.6 | 3189.2 | -67.0 ⁱ | -150.4 | -139.0 |
| $(\text{TeCF}_3)_2$ ^e | | 528.0 | 614.3 | 2321.7 ^e | 2340.2 | 2436.0 |

^a Reference 31. ^b Reference 35. ^c Reference 40. ^d Reference 43. ^e Reference 44. ^f Estimate from ref 31 based on nonrelativistic calculations. ^g Estimate from ref 31 based on relativistic calculations. ^h Reference 35. ⁱ Reference 50. ^j Revised experimental value = experimental value - 945 ppm; see text.

TABLE 2: Calculated and Experimental ^{125}Te Chemical Shifts for Various Organic Tellurium-Containing Compounds^t

| molecule | chemical shift (ppm) | | | | gross charge on Te atom (au) ^c |
|----------------------------------------------------------------------------------------------|---------------------------|----------|------------|------------|-------------------------------------------|
| | experimental ^a | δ | δ^d | δ^p | |
| $(\text{CH}_3)_2\text{Te}$ | 0 | 0 | 0 | 0 | 0.55 |
| TeH_2 ^d | ~-621 ^e | -711.4 | -4.9 | -706.5 | 0.34 |
| $\text{Te}(\text{Me}_3\text{Si})_2$ ^f | -842 ^g | -740.6 | -10.4 | -730.2 | -0.32 |
| $\text{Te}(\text{CF}_3)_2$ ^f | 1368 ^h | 1679 | 0.4 | 1678.6 | 0.50 |
| $\text{Te}_2(\text{CF}_3)_2$ ^f | 686 ^h | 996.5 | -0.6 | 997.1 | 0.34 |
| $\text{Te}_2\text{C}_5\text{H}_8\text{O}$, IV | 57.1 ^s | 331.4 | -2.1 | 333.5 | 0.22 |
| Te_2Me_2 ^f | 63 ⁱ | 257.4 | -1.9 | 259.3 | 0.24 |
| $(\text{TeCF}_2)_2$ ^j , I | 2321.7 ^j | 2436.0 | -0.45 | 2436.4 | 0.60 |
| $\text{Te}(\text{CH}_3)_4$ ^k | -67 ^l | -139.0 | 2.8 | -141.8 | 1.25 |
| $\text{TeCl}_2(\text{CH}_3)_2$ ^q | 733.8 ^r | 435.5 | 4.0 | 431.4 | 1.07 |
| $[\text{Me}_2\text{TeCl}][\text{SCONe}_2]$, V | 554.1 ^r | 227.6 | -0.5 | 228.1 | 1.03 |
| $\text{F}_2\text{Te}(\text{CF}_3)_2$ ^m | 1187 ^{h,n} | 899.6 | 3.9 | 895.7 | 1.55 |
| TeC_8H_8 ^f , II | 268 ^o | 372.5 | -0.8 | 373.3 | 0.52 |
| $\text{Te}(\text{C}_6\text{H}_4\text{N}_2\text{Ph})(\text{dmdtc})$, ^p III | 1228.6 ^p | 1111.0 | 3.3 | 1107.7 | 0.85 |

^a All data are reported with respect to Me_2Te and in solution. ^b Calculated absolute chemical shielding $\sigma_{\text{Me}_2\text{Te}} = 3050.3$ ppm, $\delta^d = 5636.3$ ppm, $\delta^p = -2586.1$ ppm, and $\delta = \sigma_{\text{Me}_2\text{Te}} - \sigma_{\text{substance}}$. ^c Atomic units. Gross charge obtained from a Mulliken population analysis. ^d Structural data from ref 45. ^e Estimated value from the relation reported given in ref 46: $\delta(^{125}\text{Te})/\delta(^{77}\text{Se}) \approx 1.8$; $\delta(^{77}\text{Se})$ of $\text{SeH}_2(\text{gas}) = -345$ ppm (ref 47). ^f Optimized structure. ^g Reference 48. ^h Reference 49. ⁱ Reference 46. ^j Reference 44. ^k Structural data from ref 43. ^l Reference 50. ^m Reference 51. ⁿ Reference 52. ^o Reference 38. ^p Reference 37. ^q Reference 66. ^r Reference 67. ^s Reference 68. ^t The structure of some of the molecules are presented in Figure 2.

for a wide range of tellurium containing compounds. We compare our results with the experimental shifts. All shifts are taken relative to $(\text{CH}_3)_2\text{Te}$ (relativistic).

^{125}Te Chemical Shifts of Organic Tellurium-Containing Complexes. The calculated ^{125}Te chemical shifts for a wide range of organic tellurium-containing compounds are presented in Table 2. The theoretical values correspond to the ^{125}Te chemical shift of a single “frozen” molecules in the gas phase at 0 K.

The calculated values are compared in Table 2 to experimental estimates. The observed ^{125}Te chemical shifts were obtained in solution at temperatures well above 0 K. Thus the experimental estimates are influenced by thermal motions and solvent effects. We estimate that these effects could amount to as much as ± 100 ppm.³⁸

Our calculated ^{125}Te chemical shifts follow the experimental trend over a range of 3000 ppm with an average deviation of 235 ppm. The deviation cannot completely be attributed to effects due to solvation and thermal motion. The largest discrepancy between theory and experiment was obtained for the fluorine-containing derivatives $(\text{CF}_3)_2\text{Te}$, $(\text{CF}_3)_2\text{Te}_2$, $\text{TeF}_2(\text{CF}_3)_2$, and $[\text{Me}_2\text{TeCl}][\text{SCONe}_2]$ (**V**), where the average deviation is 315 ppm.

Table 2 affords as well a decomposition of the ^{125}Te chemical shift

$$\delta = \sigma_{\text{Me}_2\text{Te}} - \sigma_{\text{Compound}} \quad (4)$$

into its diamagnetic

$$\delta^d = \sigma_{\text{Me}_2\text{Te}}^d - \sigma_{\text{Compound}}^d \quad (5)$$

and paramagnetic

$$\delta^p = \sigma_{\text{Me}_2\text{Te}}^p - \sigma_{\text{Compound}}^p \quad (6)$$

components as

$$\delta = \delta^d + \delta^p \quad (7)$$

where σ is the isotropic shielding constant. Further, σ^d and σ^p are respectively the diamagnetic and paramagnetic shielding constants as defined¹⁸ by the GIAO-DFT method, eq 1.

It follows from Table 2 that the total chemical shift δ is determined by the paramagnetic contribution δ^p , whereas the diamagnetic part δ^d by comparison is numerically negligible. The modest contribution from the diamagnetic shielding δ^d

TABLE 3: Calculated ^{125}Te Paramagnetic Chemical Shieldings and Orbital Energies for Various Compounds

| molecule | paramagnetic chemical shielding (ppm) (σ^p) | | orbital energy (eV) | | energy gap (eV) |
|--------------------------------------|------------------------------------------------------|-------------------------------------------|---------------------|--------------------|-----------------|
| | total ^a | contribution $\sigma^{p(\text{occ-vir})}$ | HOMO | LUMO | |
| $\text{Te}(\text{CF}_3)_2$ | -4264.7 | -4611.6 | -6.279 | -3.382 | 2.90 |
| TeC_8H_8 , II | -2959.3 | -3671.1 | -4.632 | -1.658 | 2.97 |
| $\text{Te}(\text{CH}_3)_2$ | -2586.0 | -3424.3 | -4.619 | -1.206 | 3.41 |
| TeH_2 | -1879.6 | -2316.8 | -5.594 | -1.659 | 3.94 |
| $\text{Te}(\text{Me}_3\text{Si})_2$ | -1855.9 | -1713.4 | -4.825 | -0.766 | 4.06 |
| $\text{F}_2\text{Te}(\text{CF}_3)_2$ | -3481.8 | -3406.7 | -8.159 | -3.547 | 4.61 |
| $\text{Te}(\text{CH}_3)_4$ | -2444.2 | -2968.8 | -6.822 | -0.785 | 6.04 |
| $\text{Te}_2(\text{CF}_3)_2$ | -3583.2 | -3992.8 | -6.930 | -3.890 | 3.02 |
| Te_2Me_2 | -2845.6 | -3501.9 | -5.746 (HOMO-1) | -2.727 (HOMO-1) | 3.41 |

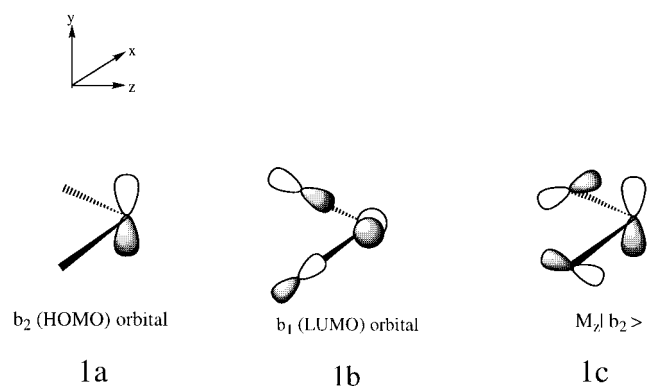
^a The total paramagnetic shielding, σ^p , consists of contributions from the coupling between occupied orbitals and virtual orbitals, $\sigma^{p(\text{occ-vir})}$, as well as terms that only depend on the occupied orbitals; see ref 18.

precludes any relation between δ and the amount of shielding electron density on tellurium, as expressed by the formal oxidation state or effective charge of this atom, Table 2.

We note that TeH_2 , $\text{Te}(\text{SiMe}_3)_2$, $\text{Te}(\text{Me}_3)_2$, $\text{Te}(\text{CF}_3)_2$, **I**, and **II** all have tellurium in the oxidation state +2 with a L–Te–L coordination where the bond angle is in the range 75.2–99.3°. Yet, these molecules have very different calculated shifts δ ranging from -740.6 ppm for $\text{Te}(\text{SiMe}_3)_2$ to 1679 ppm for $\text{Te}(\text{CF}_3)_2$ and 2436 ppm for **I**. For $(\text{Me}_3\text{Si})_2\text{Te}$, two quite different shifts of -842⁴⁸ and -43,⁵⁵ respectively, are quoted in the literature. Our DFT-GIAO calculations point to the second estimate⁵⁵ as being in error.

The chemical shift for the $\text{Te}(\text{II})\text{L}_2$ systems is seen to increase roughly with the electronegativity of L from -740.6 ppm for $\text{Te}(\text{SiMe}_3)_2$ to 1679 ppm for $\text{Te}(\text{CF}_3)_2$. This trend is in line with what one would expect from variations in the diamagnetic shielding σ^d . However, it follows from Table 2 that the chemical shift is completely dominated by the paramagnetic term δ^p , whereas the diamagnetic contribution from δ^d is negligible.

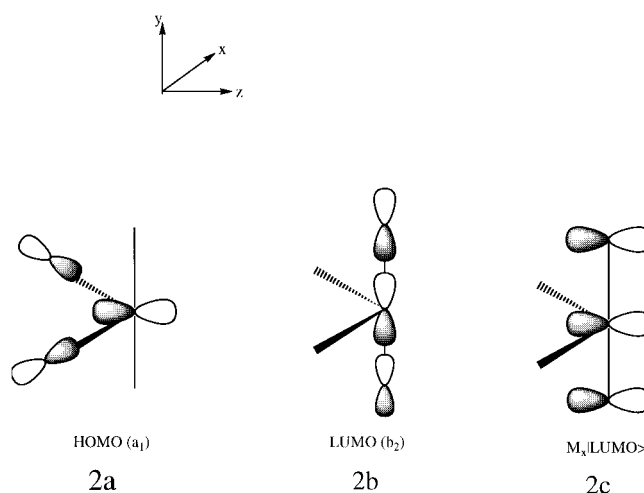
The influence of L on δ^p can be analyzed by observing that the paramagnetic contribution to the shift is due to a magnetic coupling between occupied and virtual orbitals, as indicated in eq 3. In the case of the angular $\text{Te}(\text{II})\text{L}_2$ molecules the principle paramagnetic contribution is due to the b_2 type HOMO, **1a**, which couples magnetically to the b_1 LUMO, **1b**, through the common lobes of **1a** and $\hat{M}_s|\text{LUMO}\rangle$, **1c**, eq 3. This coupling,



$u_{\text{HL}}^{(1)}$ is proportional to $\langle \text{HOMO} | \hat{M}_s | \text{LUMO} \rangle$ and inversely proportional to the HOMO–LUMO gap $\Delta\epsilon_{\text{HL}}$, eq 3. Our calculations reveal that the trend in the paramagnetic coupling is determined by $\Delta\epsilon_{\text{HL}}$. This is illustrated in Table 3, where we give calculated values for σ^p along with $\Delta\epsilon_{\text{HL}}$ and the

energies of **1a** as well as **1b**. The species $\text{Te}(\text{CF}_3)_2$ with the most electronegative substituent has the smaller $\Delta\epsilon_{\text{HL}}$ and numerically the largest σ^p and δ^p values, whereas $\text{Te}(\text{SiMe}_3)_2$ with the least electronegative substituent is found at the other end of the scale. It follows from Table 3 that both HOMO and LUMO are of lower energy in $\text{Te}(\text{CF}_3)_2$ compared to $\text{Te}(\text{SiMe}_3)_2$. However, in relative terms the LUMO **1b** is lowered more than **1a** since the former explicitly involves orbitals on the electronegative CF_3 groups, whereas the tellurium lone pair orbital **1a** only feels the electronegativity of CF_3 by induction. Hence, $\text{Te}(\text{CF}_3)_2$ has a smaller HOMO–LUMO gap and a larger chemical shift. The other $\text{Te}(\text{II})\text{L}_2$ systems have HOMO–LUMO gaps and chemical shifts between $\text{Te}(\text{SiMe}_3)_2$ and $\text{Te}(\text{CF}_3)_2$.

The calculated shifts are also far apart for the four-coordinated butterfly-shaped $\text{Te}(\text{IV})$ species with $\delta = -139$ ppm for $\text{Te}(\text{CH}_3)_4$ and $\delta = 899.6$ ppm for $\text{F}_2\text{Te}(\text{CH}_3)_2$. For these systems the important coupling is between the a_1 type HOMO, **2a**, and the b_2 LUMO, **2b**, through the common lobes in **2a** and $\hat{M}_s|\text{LUMO}\rangle$, **2c**. We note again that species with the more



electronegative substituents have the larger chemical shifts due to δ^p , Tables 2 and 3.

For the case of the angular $\text{Te}(\text{I})$ complexes with a Te–Te bond, we calculate a large shift of 996.5 ppm for $\text{Te}_2(\text{CF}_3)_2$ with the more electronegative substituents and a smaller shift of 257.4 ppm for Te_2Me_2 with the less electronegative substituents. In the case of the $\text{Te}(\text{I})$ systems the coupling is between the LUMO and the HOMO-1 orbital, Table 3. Finally, it is worth observing that the DFT-GIAO method is able to predict the ^{125}Te shift for the large size molecule $\text{Te}(\text{C}_6\text{H}_4\text{N}_2\text{Ph})(\text{dmdtc})$, **III**, to within 10%, Table 2.

^{125}Te Chemical Shifts of Inorganic Tellurium-Containing Complexes. The calculated ^{125}Te chemical shifts for a wide range of inorganic tellurium-containing compounds are presented in Table 4. Also the diamagnetic (δ^d) and paramagnetic (δ^p) contributions to the chemical shift as well as the gross charge on the tellurium atom are shown.

The calculated values are compared in Table 4 with experimental data. Our calculated ^{125}Te chemical shifts follow the experimental trend over a range of 3400 ppm with an average deviation of 160 ppm. The deviation could be attributed to the influence of thermal motion and for the ionic species also to solvation effects. The larger discrepancy between theory and experiment was obtained for $[\text{TeCl}_6]^{2-}$, TeS_3^{2-} , and $[\text{Te}_6]^{4+}$, where the average deviation is 253 ppm.

It is the paramagnetic contribution δ^p that determines the total chemical shift δ , whereas the diamagnetic part δ^d by comparison

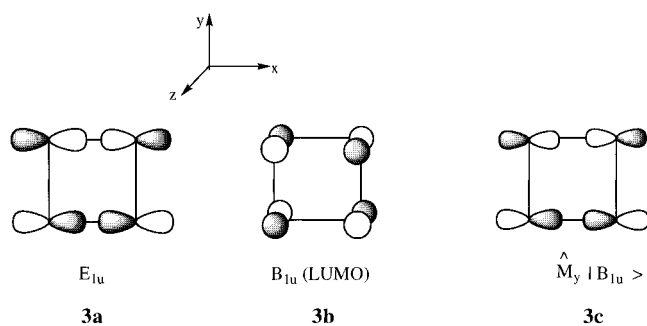
TABLE 4: Calculated and Experimental ^{125}Te Chemical Shifts for Various Inorganic Tellurium-Containing Compounds

| molecule | experimental ^a | chemical shift (ppm) | | | gross charge on Te atom (au) ^e |
|--------------------------------------------|---------------------------------------------|----------------------|-------------------------|-------------|-------------------------------------------|
| | | δ | calculated ^b | δ^p | |
| $[\text{Te}_6]^{4+}$ (cyclic) ^d | 148 ^{cf} | -230.0 | -1.6 (av) | -228.4 (av) | 0.67 |
| $\text{Te}=\text{P}(\text{Pr})_3^j$ | -1000.3 ^r | -792.9 | -4.9 | -788.0 | 0.26 |
| $\text{Te}=\text{P}(\text{CH}_3)_3^j$ | -513.4 ^k | -247.3 | -6.9 | -240.4 | -0.30 |
| $\text{CH}_3\text{OTeF}_6^{-q}$ | 374.2 ^{f,q} | 483.9 | 1.7 | 482.2 | 3.12 |
| TeF_6^d | 545 ^s | 602.0 | 5.5 | 596.6 | 3.41 |
| $\text{Te}(\text{OH})_6^l$ | 707 (in H_2O) ^m | 644.9 | 0.9 | 644 | 2.9 |
| | 712 (in H_2O) ⁿ | | | | |
| $[\text{TeCl}_6]^{2-d}$ | 1531 ^s | 1313.0 | 6.6 | 1306.4 | 1.08 |
| $[\text{TeBr}_6]^{2-d}$ | 1348 ^s | 1335.7 | 3.1 | 1332.6 | 0.95 |
| TeS_3^{2-o} | 1514 ^p | 1711.4 | -2.9 | 1714.3 | 0.61 |
| $[\text{Te}_4]^{2+}$ (cyclic) ^d | 2665-2625 ^h | 2544.2 | -3.4 (av) | 2547.5 (av) | 0.50 |

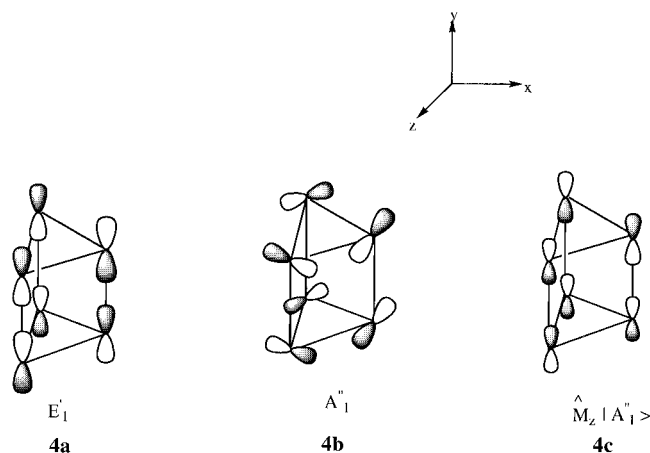
^a All data are reported with respect to Me_2Te and in solution. ^b Calculated absolute chemical shielding $\sigma_{\text{Me}_2\text{Te}} = 3050.3$ ppm, $\sigma^d = 5636.3$ ppm, $\sigma^p = -2586.1$ ppm, and $\delta = \sigma_{\text{Me}_2\text{Te}} - \sigma_{\text{substance}}$. ^c Atomic units. ^d Gross charge calculated from a Mulliken population analysis. ^e Structural data from ref 40. ^f Reference 58. ^g The experimental data originally reported in ppm relative to $\text{Te}(\text{OH})_6$ have been converted using the experimental shift of $\text{Te}(\text{OH})_6$ relative to Me_2Te $\delta = 707$ ppm.⁵⁹ ^h Reference 38. ⁱ Concentration dependent, ref 60. ^j Reference 61. ^k Reference 54. ^l Reference 62. ^m Reference 59. ⁿ Reference 63. ^o Reference 64. ^p Reference 65. ^q Reference 69. ^r Reference 70.

is numerically negligible, Table 4. The modest contribution from the diamagnetic shielding, δ^d , precludes any relation between δ and the amount of shielding electron density on tellurium, as expressed by the formal oxidation state or effective charge of this atom, Table 4.

It is beyond the scope of this study to provide an analysis of the factors contributing to δ^p for each of the compounds in Table 4. However, we shall as an example briefly analyze $[\text{Te}_6]^{4+}$ and $[\text{Te}_4]^{2+}$ since these two pure tellurium compounds have quite different calculated chemical shifts of -230 and 2544.2 ppm, respectively. For the case of $[\text{Te}_4]^{2+}$ the paramagnetic shielding comes mainly from the coupling between the occupied orbitals $5E_{1u}$, **3a**, and the LUMO ($2B_{1u}$), **3b**, through the common lobes of $\hat{M}_z | B_{1u} \rangle$, **3c**. On the other hand, the



paramagnetic shielding in $[\text{Te}_6]^{4+}$ is due to the coupling between the occupied orbitals $8E'_1$, **4a**, and the virtual orbital $3A''_1$, **4b**, through the common lobes $\hat{M}_z | A_1'' \rangle$, **4c**. The species $[\text{Te}_4]^{2+}$

**TABLE 5: Calculated ^{125}Te Paramagnetic Chemical Shifts and Chemical Shieldings for Various Inorganic Tellurium-Containing Compounds**

| molecule | δ^p paramagnetic shift (ppm) | σ^p paramagnetic shielding (ppm) | | |
|----------------------|-------------------------------------|-----------------------------------------|--------------------|-----------------|
| | | σ^p total | σ^p OCC-VIR | energy gap (eV) |
| $[\text{Te}_6]^{4+}$ | -228.4 | -2357.4 | -3007.4 | 3.8 |
| $[\text{Te}_4]^{2+}$ | 2547.5 | -5136.5 | -5501.1 | 3.3 |

has in the first place the stronger paramagnetic shielding as a result of a smaller energy gap between the two orbitals involved, Table 5. In addition, the induced current density \vec{J}^p is spread over only four centers in $[\text{Te}_4]^{2+}$ as opposed to six in the case of $[\text{Te}_6]^{4+}$. This means that the amplitude of \vec{J}^p around each Te center at a given distance r_N is larger in $[\text{Te}_4]^{2+}$ than in $[\text{Te}_6]^{4+}$. Since the \vec{J}^p contribution to σ^p decays as $(1/r_N)^2$, eq 1, one would expect that $[\text{Te}_4]^{2+}$ with the larger amplitude of \vec{J}^p around the NMR probe numerically has the larger paramagnetic shielding σ^p .

^{125}Te Chemical Shifts of Organometallic Tellurium-Containing Complexes. The calculated ^{125}Te chemical shifts for a wide range of organometallic tellurium-containing compounds are presented in Table 6. Our calculated ^{125}Te chemical shifts follow the experimental trend over a range of 2400 ppm with an average deviation of 155 ppm. Again, it is the paramagnetic contribution, δ^p , rather than the diamagnetic contribution, δ^d , that determines the total chemical shift δ , Table 6.

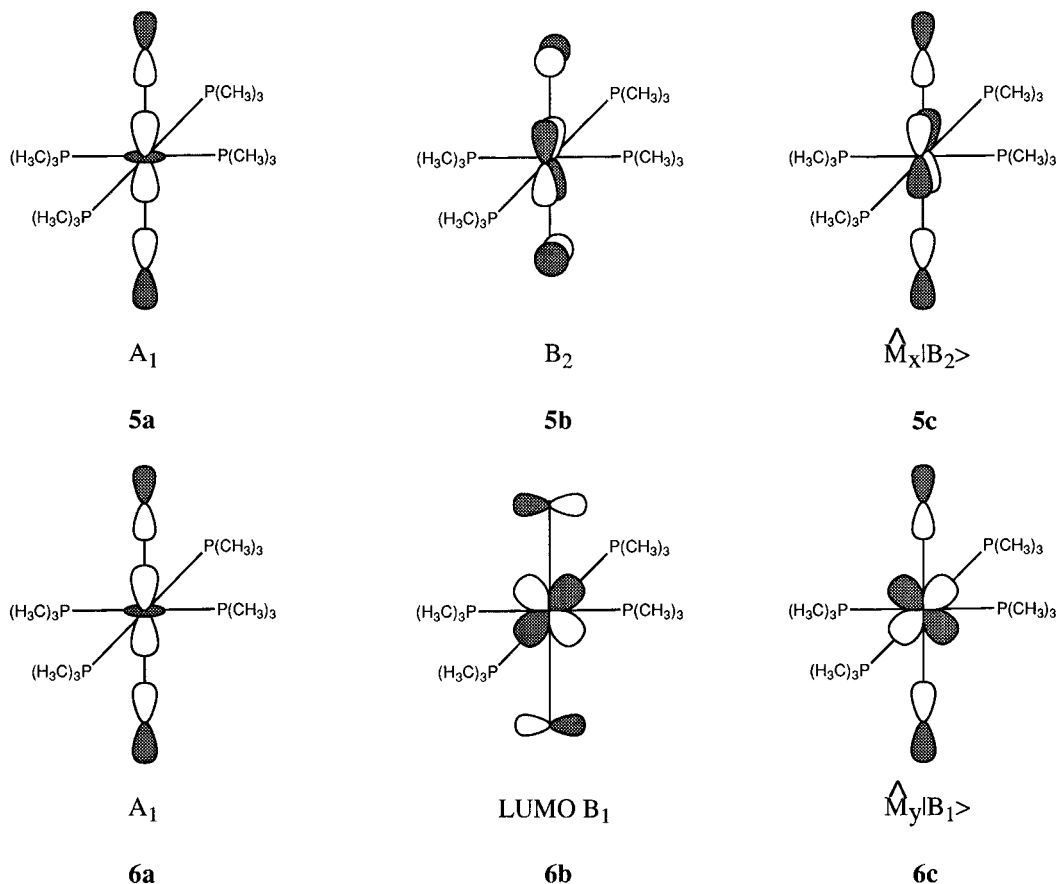
The chemical shift of $[\text{Cp}^*\text{Re}(\text{CO})_2\text{H}(\text{TeH})]$ is negative, and the GIAO-DFT method is able to predict a chemical shift that is comparable with the experimental estimate. The observed shift of $\delta = -901.3$ ppm indicates that the magnetic environment of the tellurium is similar to that found in TeH^- , for which a ^{125}Te NMR chemical shift of -1393.0 ppm was calculated. The corresponding experimental value for TeH^- ranges from -919 to -1209 ppm in solution.⁶¹ The magnetic environment of the tellurium atom is also quite similar for the $\text{Te}(\text{CH}_2)_4$ ligand in the free state and in the complex $\text{trans}[\text{Pd}\{\text{Te}(\text{CH}_2)_4\}_2\text{Cl}_2]$, **VIII**. We calculate a chemical shift of 566 ppm for **VIII** compared to 607 ppm for free $\text{Te}(\text{CH}_2)_4$.

The compound $\text{Fe}_2(\text{CO})_6(\mu\text{-TeMe})_2$, **VII**, contains $[\text{TeCH}_3]^-$ as a ligand. The absolute chemical shielding of free $[\text{TeCH}_3]^-$ is calculated to be 3209 ppm, which is similar to the calculated absolute chemical shielding of $\text{Te}(\text{CH}_3)_2$ (3050.3 ppm). The paramagnetic coupling that gives rise to the chemical shift in

TABLE 6: Calculated and Experimental ^{125}Te Chemical Shifts for Various Organometallic Tellurium-Containing Compounds^h

| molecule | experimental ^a | chemical shift (ppm) | | | gross charge on Te atom (au) ^d |
|--------------------------------------------------------------------------------------------------|---------------------------|-------------------------|------------|------------|-------------------------------------------|
| | | calculated ^c | | | |
| | | δ | δ^d | δ^p | |
| $\text{Mo}(\text{PMe}_3)_4(\text{Te})_2$, ⁱ VI | 1507 | 1240.6 | -7.4 | 1247.8 | -0.50 |
| $\text{W}(\text{PMe}_3)_4(\text{Te})_2$, ^g VI | 950 | 905.4 | -5.7 | 911 | -0.35 |
| $\text{Fe}_2(\text{CO})_6(\mu\text{-TeMe})_2$, ^j VII | 20 | 112.5 | 0.3 | 112.2 | 0.30 |
| <i>trans</i> - $[\text{Pd}\{\text{Te}(\text{CH}_2)_4\}_2\text{Cl}_2]$, ^k VIII | 484 | 607.2 | -0.4 | 607.6 | 0.70 |
| $[\text{Cp}^*\text{Re}(\text{CO})_2\text{H}(\text{TeH})]$, ^l IX | -901.3 | -650.6 | 0.9 | -651.5 | 0.29 |

^a All data are reported with respect to Me_2Te and in solution. ^b The data originally reported with respect to $\text{Te}(\text{OH})_6$ have been converted using the experimental chemical shift of $\text{Te}(\text{OH})_6$ of 707 ppm. ^c Calculated absolute chemical shielding $\sigma_{\text{Me}_2\text{Te}} = 3050.3$ ppm, $\delta^d = 5636.3$ ppm, $\delta^p = -2586.1$ ppm, and $\delta = \sigma_{\text{Me}_2\text{Te}} - \sigma_{\text{substance}}$. ^d Atomic units. Gross charge calculated from a Mulliken population analysis. ^e Reference 41. ^f Reference 42. ^g Reference 56. ^h The structures of the complexes are presented in Figure 3. ⁱ Reference 72. ^j Reference 73. ^k Reference 74. ^l Reference 75.



the complex $\text{Fe}_2(\text{CO})_6(\mu\text{-TeMe})_2$ is thought to be similar to that discussed for $\text{Te}(\text{CH}_3)_2$ in structures **1a–1c**.

The complexes $\text{M}(\text{PMe}_3)_4(\text{Te})_2$ ($\text{M} = \text{Mo}, \text{W}$), **VI**, contain two Te atoms as ligands. The chemical shift calculated for these complexes, Table 6, indicates that the magnetic environment of the Te atom in the complexes is different from that of the free atom. In the free atom only the diamagnetic contribution determines the chemical shift, while in the complex it is the paramagnetic contribution that determines the chemical shift. The calculated chemical shift for the free atom is -2589.8 ppm. There are two main types of paramagnetic couplings that give rise to the chemical shift in these complexes. The first involves the occupied A_1 orbital, **5a**, and the virtual B_2 , **5b**, orbital. The orbital $\hat{M}_x|B_2\rangle$, **5c**, will overlap with A_1 , **5a**, through the common lobes on **5a** and **5c**. The second involves the same occupied orbital A_1 , **6a**, and the LUMO (B_1), **6b**. The occupied orbital A_1 , **6a**, can couple with the empty LUMO orbital, **6b**, since $\hat{M}_y|LUMO\rangle$, **6c**, has common lobes with A_1 , **6a**. These types of paramagnetic coupling are similar to those found in metal hexacarbonyls in which a paramagnetic coupling between the

σ_{CO} HOMO and the π^*_{CO} LUMO of CO through the overlaps $\langle\sigma_{\text{CO}}|\hat{M}_s|\pi^*_{\text{CO}}\rangle$, with $s = x, y$, is observed.³³

4. Conclusions

Calculations were carried out on the ^{125}Te NMR chemical shifts for a number of organic, inorganic, and organometallic tellurium-containing complexes. The calculated shifts span a range of about 3000 ppm and therefore cover almost the complete range of known ^{125}Te chemical shifts. It was found that the DFT-GIAO method is able to predict ^{125}Te NMR chemical shifts that follow the same trends as experiment. This is—to our knowledge—the first time that ^{125}Te NMR chemical shifts have been studied systematically by a first-principles electronic structure theory with the inclusion of relativity.

Acknowledgment. This work has been supported by the National Sciences and Engineering Research Council of Canada (NSERC). G.S. acknowledges the Graduate Faculty Council, University of Calgary, for a scholarship, Y. R.-M. acknowledges a scholarship from DGAPA-UNAM (Mexico), and T.Z. ac-

knowledges a Canada Council Killam Research Fellowship. Y. R.-M. is grateful to Dr. W. Piers for the helpful and enjoyable literature. We would like to thank the Petroleum Research Fund, administered by American Chemical Society (ACS-PRF No. 31205-AC3), for further support of this research.

References and Notes

- (1) Fukui, H. *Magn. Reson. Rev.* **1987**, *11*, 205.
- (2) Chesnut, D. B. In *Annual Reports on NMR Spectroscopy*; Webb, G. A., Ed.; Academic Press: New York, 1989; Vol. 21.
- (3) Chesnut, D. B. In *Annual Reports on NMR Spectroscopy*; Webb, G. A., Ed.; Academic Press: New York, 1994; Vol. 29.
- (4) Tossell, J. A., Ed. *Nuclear Magnetic Shieldings and Molecular Structure, NATO ASI C386*; Kluwer Academic Publishers: Dordrecht, The Netherlands, 1993.
- (5) Kutzelnigg, W.; Fleischer, U.; Schindler, M. In *NMR-Basic Principles and Progress*; Springer-Verlag: Berlin, 1990; Vol. 23, p 165.
- (6) Jameson, C. J. In *Specialist Periodic Reports on NMR*; Webb, G. A., Ed.; Royal Society of Chemistry: London, 1980–1994, Vols. 8–24.
- (7) Gauss, J.; Stanton, J. F. *J. Chem. Phys.* **1995**, *102*, 251.
- (8) Gauss, J.; Stanton, J. F. *J. Chem. Phys.* **1996**, *104*, 2574.
- (9) Mason, J. Ed. *Multinuclear NMR*; Plenum Press: New York, 1987.
- (10) Nakatsuji, H. In *Nuclear Magnetic Shieldings and Molecular Structure, NATO ASI C386*; Tossell, J. A., Ed.; Kluwer Academic Publishers: Dordrecht, The Netherlands, 1993; p 263.
- (11) Kaupp, M.; Malkin, V. G.; Malkina, O. L.; Salahub, D. R. *J. Am. Chem. Soc.* **1995**, *117*, 1851.
- (12) Kaupp, M.; Malkin, V. G.; Malkina, O. L.; Salahub, D. R. *Chem. Phys. Lett.* **1995**, *235*, 382.
- (13) Berger, S.; Bock, W.; Frenking, G.; Jonas, V.; Müller, F. *J. Am. Chem. Soc.* **1995**, *117*, 1851.
- (14) Ellis, P. D.; Odom, J. D.; Lipton, A. S.; Chen, Q.; Gulick, J. M. In *Nuclear Magnetic Shieldings and Molecular Structure, NATO ASI C386*; Tossell, J. A., Ed.; Kluwer Academic Publishers: Dordrecht, The Netherlands; 1993, p 539.
- (15) Ellis, P. D.; Odom, J. D.; Lipton, A. S.; Gulick, J. M. *J. Am. Chem. Soc.* **1993**, *115*, 755.
- (16) Pyykkö, P. *Chem. Rev.* **1988**, *88*, 563.
- (17) Pyykkö, P. In *The Effect of Relativity on Atoms, Molecules, and the Solid State*; Wilson, S., Ed.; Plenum Press: New York; 1991; p 1.
- (18) Schreckenbach, G.; Ziegler, T. *J. Phys. Chem.* **1995**, *99*, 606.
- (19) (a) Schreckenbach, G.; Dickson, R. M.; Ruiz-Morales, Y.; Ziegler, T. In *Density Functional Theory in Chemistry*; Laird, B., Ross, R.; Ziegler, T., Eds.; American Chemical Society: Washington, DC, 1996; p 328. (b) Ballhausen, C. J. In *Introduction to Ligand Field Theory*; McGraw-Hill: New York, 1962; p 149. (c) McGlynn, S. P.; Vanquickenborne, L. G.; Kinoshita, M.; Carroll, D. G. In *Introduction to Applied Quantum Chemistry*; Holt, Rinehart and Winston: New York, 1972.
- (20) Schreckenbach, G.; Ruiz-Morales, Y.; Ziegler, T. *J. Chem. Phys.* **1996**, *104*, 8605.
- (21) Schreckenbach, G.; Ziegler, T. *Int. J. Quantum Chem.* **1996**, *60*, 753.
- (22) Schreckenbach, G.; Ziegler, T. *Int. J. Quantum Chem.*, in press.
- (23) Baerends, E. J.; Ellis, D. E.; Ros P. *Chem. Phys.* **1973**, *2*, 41.
- (24) Baerends, E. J.; Ros, P. *Chem. Phys.* **1973**, *2*, 52.
- (25) Baerends, E. J. Ph.D. Thesis, Free University, Amsterdam, The Netherlands, 1973.
- (26) Baerends, E. J.; Ros P. *Int. J. Quantum Chem. Symp.* **1978**, *12*, 169.
- (27) te Velde G.; Baerends E. J. *Int. J. Quantum Chem.* **1988**, *33*, 87.
- (28) te Velde G. *Amsterdam Density Functional (ADF), User Guide, Release 1.1.3*; Department of Theoretical Chemistry, Free University: Amsterdam, The Netherlands, 1994.
- (29) Becke, A. *Phys. Rev.* **1988**, *A38*, 3098.
- (30) Perdew, J. *Phys. Rev.* **1986**, *B33*, 8822.
- (31) Jameson, C. J.; Jameson, A. K. *Chem. Phys. Lett.* **1987**, *135*, 254.
- (32) Blom, R.; Haaland, A.; Seip, R. *Acta Chem. Scand.* **1983**, *A37*, 595.
- (33) Ruiz-Morales, Y.; Schreckenbach, G.; Ziegler T. *J. Phys. Chem.* **1996**, *100*, 3359.
- (34) Vernoijs, P.; Snijders, J. G.; Baerends, E. J. *Slater Type Basis Functions for the Whole Periodic Table*; Internal report (in Dutch); Department of Theoretical Chemistry, Free University: Amsterdam, The Netherlands, 1981.
- (35) Blom, R.; Haaland, A. and Seip, R. *Acta Chem. Scand.* **1983**, *A37*, 595.
- (36) McWhinnie W. R. In *Encyclopedia of Inorganic Chemistry*; King, R. B., Ed.; John Wiley and Sons Ltd.: Chichester, England, 1994; Vol. 8, pp 4117–4133.
- (37) Ahmed, M. A. K.; McCarthy, A. E.; McWhinnie, W. R.; Berry, F. *J. Chem. Soc., Dalton Trans.* **1986**, 771.
- (38) McFarlane, H. C. E.; McFarlane, W. In *Multinuclear NMR*; Mason, J., Ed.; Plenum: New York, 1987; p 417.
- (39) Björgvinsson, M.; Sawyer, J. F.; Schrobilgen, G. J. *Inorg. Chem.* **1991**, *30*, 4238.
- (40) McWhinnie, W. R. In *Encyclopedia of Inorganic Chemistry*; King, R. B., Ed.; John Wiley and Sons Ltd.: Chichester, England, 1994; Vol. 8, pp 4105–4116.
- (41) Flomer, W. A.; O'Neal, S. C.; Kolis, J. W.; Jeter, D.; Cordes, A. W. *Inorg. Chem.* **1988**, *27*, 971.
- (42) Flomer, W. A.; Kolis, J. W. *Inorg. Chem.* **1989**, *28*, 2513.
- (43) Blake, A. J.; Pulham, C. R.; Greene, T. M.; Downs, A. J.; Haaland, A.; Verne, H. P.; Volden, H. V.; Marsden, J. C.; Smart, B. A. *J. Am. Chem. Soc.* **1994**, *116*, 6043.
- (44) Boese, R.; Haas, A.; Limberg, C. *J. Chem., Soc., Chem. Commun.* **1991**, 1378.
- (45) Moncur, N. K.; Willson, P. D.; Edwards, T. H. *J. Mol. Spectrosc.* **1974**, *52*, 380.
- (46) McFarlane, H. C.; McFarlane, W. *J. Chem. Soc., Dalton Trans.* **1973**, 2416.
- (47) Duddeck, H. *Prog. NMR Spectrosc.* **1995**, *27*, 1.
- (48) Jones, C. H. W.; Sharma, R. D.; Taneja, S. P. *Can. J. Chem.* **1986**, *64*, 980.
- (49) Gombler, W. Z. *Naturforsch.* **1981**, *36b*, 535.
- (50) Gedridge, R. W., Jr.; Harris, D. C.; Higa, K. T.; Nissan, R. A. *Organomet.* **1989**, *8*, 2817.
- (51) Preut, H.; Wilkes, B.; Naumann, D. *Acta Crystallogr.* **1990**, *C46*, 1113.
- (52) Naumann, D.; Herberg, S. *J. Fluorine Chem.* **1976**, *8*, 1977.
- (53) Sandblom, N.; Ziegler, T.; Chivers, T. *Can. J. Chem.*, accepted.
- (54) Kuhn, N.; Henkel, G.; Schuman, H.; Fröhlich, R. *Z. Naturforsch.* **1990**, *45b*, 1010.
- (55) DuMont, W. W. and Kroth, H.-J. *Z. Naturforsch. B, Anorg. Chem. Org. Chem.* **1981**, *36B*, 332.
- (56) Ravinovich, D.; Parkin, G. *Inorg. Chem.* **1995**, *34*, 6341–6361.
- (57) Murphy, V. J.; Ravinovich, D.; Halkyard, S.; Parkin, G. *J. Chem. Soc., Chem. Commun.* **1995**, 1099.
- (58) Schrobilgen, G. J.; Burns, R. C.; Granger, P. *J. Chem. Soc., Chem. Commun.* **1978**, 957.
- (59) Tötsch, W.; Peringer, P.; Sladky, F. *J. Chem. Soc., Chem. Commun.* **1981**, 841.
- (60) Lassigne, C. R.; Wells, E. J. *J. Chem. Soc., Chem. Commun.* **1978**, 956.
- (61) Batchlor, R. J.; Einstein, F. W. B.; Gay, I. D.; Jones, H. W.; Sharma, R. D. *Inorg. Chem.* **1993**, *32*, 4378.
- (62) Ilczyszyn, M. M.; Lis, T.; Baran, J.; Ratajczak, H. *J. Mol. Struct.* **1992**, *265*, 293.
- (63) Gindelberger, D. E.; Arnold, J. *Organometallics* **1994**, *13*, 4462.
- (64) Bubenheim, W.; Frenzel, G.; Muller, Z. *Anorg. Allg. Chem.* **1994**, *620*, 1046.
- (65) Björgvinsson, M.; Sawyer, J. F.; Schrobilgen, G. J. *Inorg. Chem.* **1991**, *30*, 4238.
- (66) Ziolo, R. F.; Troup, J. M. *J. Am. Chem. Soc.* **1983**, *105*, 229.
- (67) Drake, J. E.; Khasrou, L. N.; Mislankar, A. G.; Ratnani, R. *Inorg. Chem.* **1994**, *33*, 6154.
- (68) Lakshminantham, M. V.; Cava, M. P.; Gunther, W. H. H.; Nugara, P. N.; Belmore, K. A.; Atwood, J. L.; Cragg, P. *J. Am. Chem. Soc.* **1993**, *115*, 885.
- (69) Mahjoub, A.-R.; Drews, T.; Seppelt, K. *Angew. Chem., Int. Ed. Engl.* **1992**, *31*, 1036.
- (70) Kuhn, N.; Henkel, G.; Schumman, H.; Fröhlich, R. *Z. Naturforsch.* **1990**, *45b*, 1010.
- (71) The bracket notation $\langle \Psi_1 | M_Z | \Psi_2 \rangle$ denotes certain matrix elements (integrals) between the two orbitals Ψ_1 and Ψ_2 that contribute to the paramagnetic shielding σ^p .
- (72) Murphy, V. J.; Parkin, G. *J. Am. Chem. Soc.* **1995**, *117*, 3522.
- (73) Kemmitt, T.; Levason, W.; Oldroyd, R. D.; Webster, M. *Polyhedron* **1992**, *11*, 2165.
- (74) Herrmann, W. A.; Hecht, C.; Herdtweck, E.; Kneuper, H.-J. *Angew. Chem., Int. Ed. Engl.* **1987**, *26*, 132.
- (75) Bachman, R. E. Whitmire, K. H. *Organometallics* **1993**, *12*, 1988.